THE 2022 TECHMED EVENT

Quantitative contrast-enhanced ultrasound imaging of breast cancer

Massimo Mischi
Eindhoven University of Technology

EINDHOVEN UNIVERSITY OF TECHNOLOGY
biomedical diagnostics
THE 2022 TECHMED EVENT

Breast cancer

Leading Sites of New Cancer Cases and Deaths 2022 Estimates

Incidence:

no. 1 for cancer cases in women (31%)

Mortality:

no. 2 for cancer deaths in women (15%)

Female

Breast	287,850	31%
Lung & bronchus	118,830	13%
Colon & rectum	70,340	8%
Uterine corpus	65,950	7%
Melanoma of the skin	42,600	5%
Non-Hodgkin lymphoma	36,350	4%
Thyroid	31,940	3%
Pancreas	29,240	3%
Kidney & renal pelvis	28,710	3%
Leukemia	24,840	3%
All sites	**934,870**	

Female

Lung & bronchus	61,360	21%
Breast	43,250	15%
Colon & rectum	24,180	8%
Pancreas	23,860	8%
Ovary	12,810	4%
Uterine corpus	12,550	4%
Liver & intrahepatic bile duct	10,100	4%
Leukemia	9,980	3%
Non-Hodgkin lymphoma	8,550	3%
Brain & other nervous system	7,570	3%
All sites	**287,270**	

Diagnostics and screening

American Cancer Society®

Screening by mammography + lesion biopsy

12% suspicious of which 4% positive → many unnecessary biopsies

MRI advised for high-risk groups

Complemented by B-mode ultrasound

Challenge: lesion classification

- Elastography[1]
- Doppler[2]
- CEUS[3,4]
- Multiparametric[5,6]

[1] Zhi et al. *Academic Radiology* 2010

[2] Stanzani et al. *Clinics* 2014

[3] Wang et al. *European Radiol* 2016

[4] Zhao et al. OncoTargets and Therapy 2017

[5] Kapetas et al. *Invest Radiol* 2019

[6] Li et al. *UMB* 2020

Objective: CEUS imaging of breast cancer

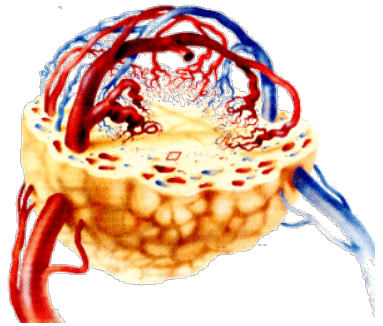

Cancer angiogenesis

Rationale: cancer growth requires angiogenesis

Angiogenic microvasculature shows **increased**

- Density
- Tortuosity
- Irregularity
- Arteriovenous shunting

Folkman et al. *Nature* 1989
Brawer et al. *J Cell Biochem* 1992
Weidner et al. *Am J Pathology* 1993
Russo et al. *BJU Int* 2012

CEUS features of breast cancer

CEUS enhancement pattern	Malignant, n (%)	Benign, n (%)	χ^2	P
Distribution of contrast agent*			44.389	0.000
Homogeneous	3 (6.8)	46 (62.2)		
Heterogeneous	37 (84.1)	22 (29.7)		
Partial enhancement with perfusion defect	3 (6.8)	2 (2.7)		
Contour enhancement	1 (2.3)	4 (5.4)		
Enhancement time*			22.300	0.000
Earlier	39 (88.6)	34 (45.9)		
Synchronous	5 (11.4)	38 (51.4)		
Later	0	2 (2.7)		
Enhanced intensity*			58.257	0.000
Hypo-enhancement	1 (2.2)	19 (25.7)		
Iso-enhancement	5 (11.4)	44 (59.5)		
Hyper-enhancement	38 (86.4)	11 (14.9)		
Enhanced area enlargement*			67.266	0.000
None	2 (4.5)	61 (82.4)		
Yes	42 (95.5)	13 (17.6)		
Presence of radial or penetrating vessels*			58.092	0.000
None	6 (13.6)	63 (85.1)		
Yes	38 (86.4)	11 (14.9)		
Margin of enhanced lesion*			34.415	0.000
Clear	6 (13.6)	40 (54.1)		
Less clear	12 (27.3)	26 (35.1)		
Unclear	26 (59.1)	8 (10.8)		

*, statistical significance. CEUS, contrast-enhanced ultrasound.

Liu et al. *Gland Surgery* 2019

Heterogenous/irregular hyperenhancement → malignancy

Table 1
Comparison of enhancement patterns between benign and malignant breast lesions.

Enhancement patterns	Benign ($n = 41$)	Malignant ($n = 86$)	*P* value
Enhancement degree			<0.001
Hypo-enhancement/iso-enhancement	33(80.5%)	32(37.2%)	
Hyper-enhancement	8(19.5%)	54(62.8%)	
Enhancement order			<0.001
Centrifugal/diffused	31(75.6%)	26(30.2%)	
Centripetal	10(24.4%)	60(69.8%)	
Internal homogeneity			<0.001
Homogeneous	29(70.7%)	22(25.6%)	
Heterogeneous	12(29.3%)	64(74.4%)	
Enhancement margin			<0.001
Well defined	25(61.0%)	18(20.9%)	
Poorly defined	16(39.0%)	68(79.1%)	
Enhancement shape			0.021*
Regular	16(39.0%)	17(19.8%)	
Irregular	25(61.0%)	69(80.2%)	
Perfusion defects			<0.001
Absent	36(87.8%)	45(52.3%)	
Present	5(12.2%)	41(47.7%)	
Surrounding vessels			<0.001
Absent	33(80.5%)	33(38.4%)	
Present	8(19.5%)	53(61.6%)	
Diameter			0.003
Not enlarged	35(85.4%)	51(59.3%)	
Enlarged	6(14.6%)	35(40.7%)	

* Enhancement shape ($P = 0.021$) will not be significant after Bonferroni Correction.

Wang et al. *European Radiol* 2016

15 years of research on prostate cancer…

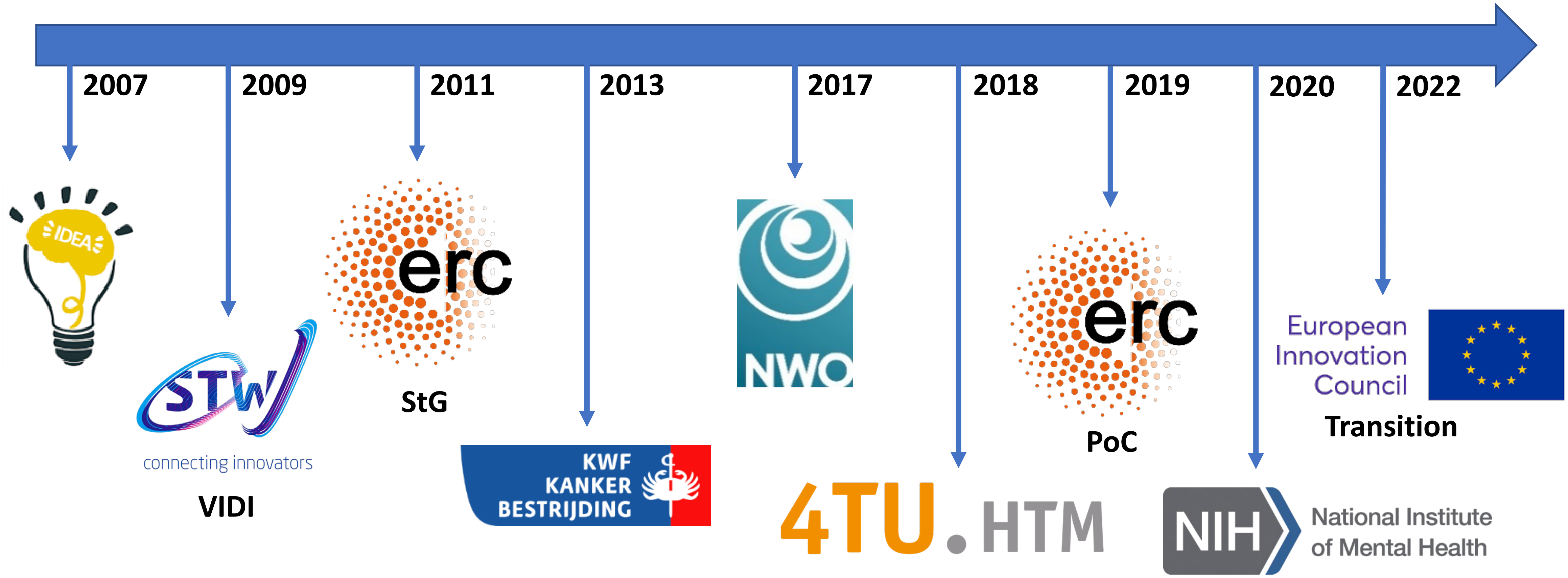

Contrast Ultrasound Dispersion Imaging (CUDI)

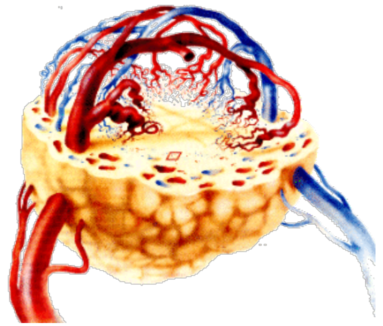

Cancer angiogenesis

Prostate CEUS

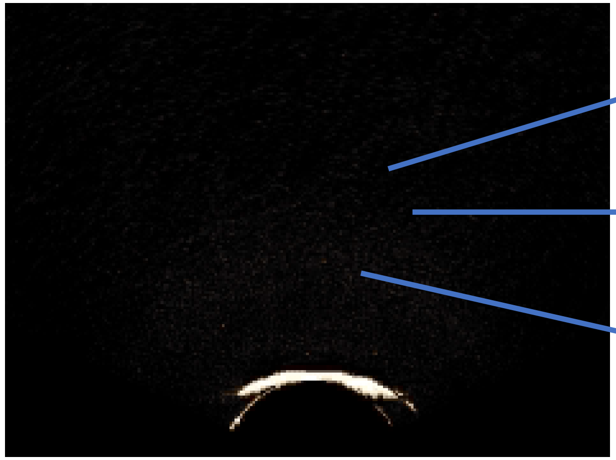

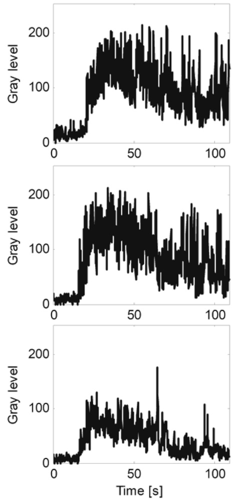

Time intensity curves

Convective dispersion modeling

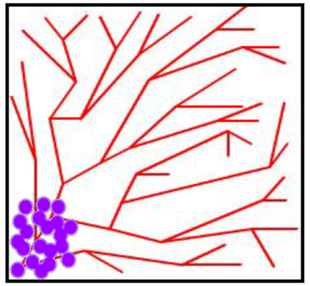

$$\partial_t C = \nabla \cdot \boldsymbol{D}\nabla C - \vec{v} \cdot \nabla C$$

$$C(t) = \alpha\sqrt{\frac{\kappa}{2\pi t}}\exp\left(-\frac{\kappa}{2t}(t-\mu)^2\right)$$

Dispersion map ⟷ Microvascular architecture

Contrast Ultrasound Dispersion Imaging (CUDI)

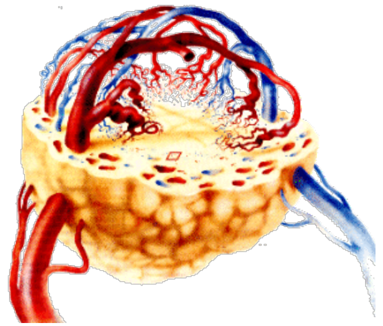

Cancer angiogenesis

Dispersion estimators

Kuenen *et al*. *IEEE T-MI* 2011
Mischi *et al*. *IEEE T-UFFC* 2012
Kuenen *et al*. *IEEE UMB* 2013
Kuenen *et al*. *IEEE T-UFFC* 2013
Kuenen et al. *IEEE T-BME* 2014
Schalk et al. *IEEE T-UFFC* 2015
Schalk *et al*. *IEEE T-BME* 2017
van Sloun et al. *Med Im Analysis* 2017
van Sloun et al. *IEEE T-MI* 2017
Wildeboer et al. *IEEE T-MI* 2018

Convective dispersion modeling

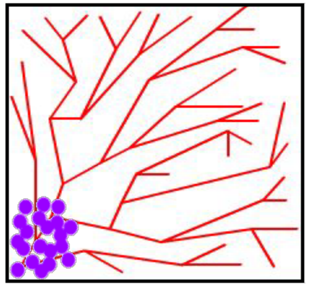

$$\partial_t C = \nabla \cdot \boldsymbol{D} \nabla C - \vec{v} \cdot \nabla C$$

$$C(t) = \alpha \sqrt{\frac{\kappa}{2\pi t}} \exp\left(-\frac{\kappa}{2t}(t-\mu)^2\right)$$

Dispersion map ⟷ Microvascular architecture

Contrast Ultrasound Dispersion Imaging (CUDI)

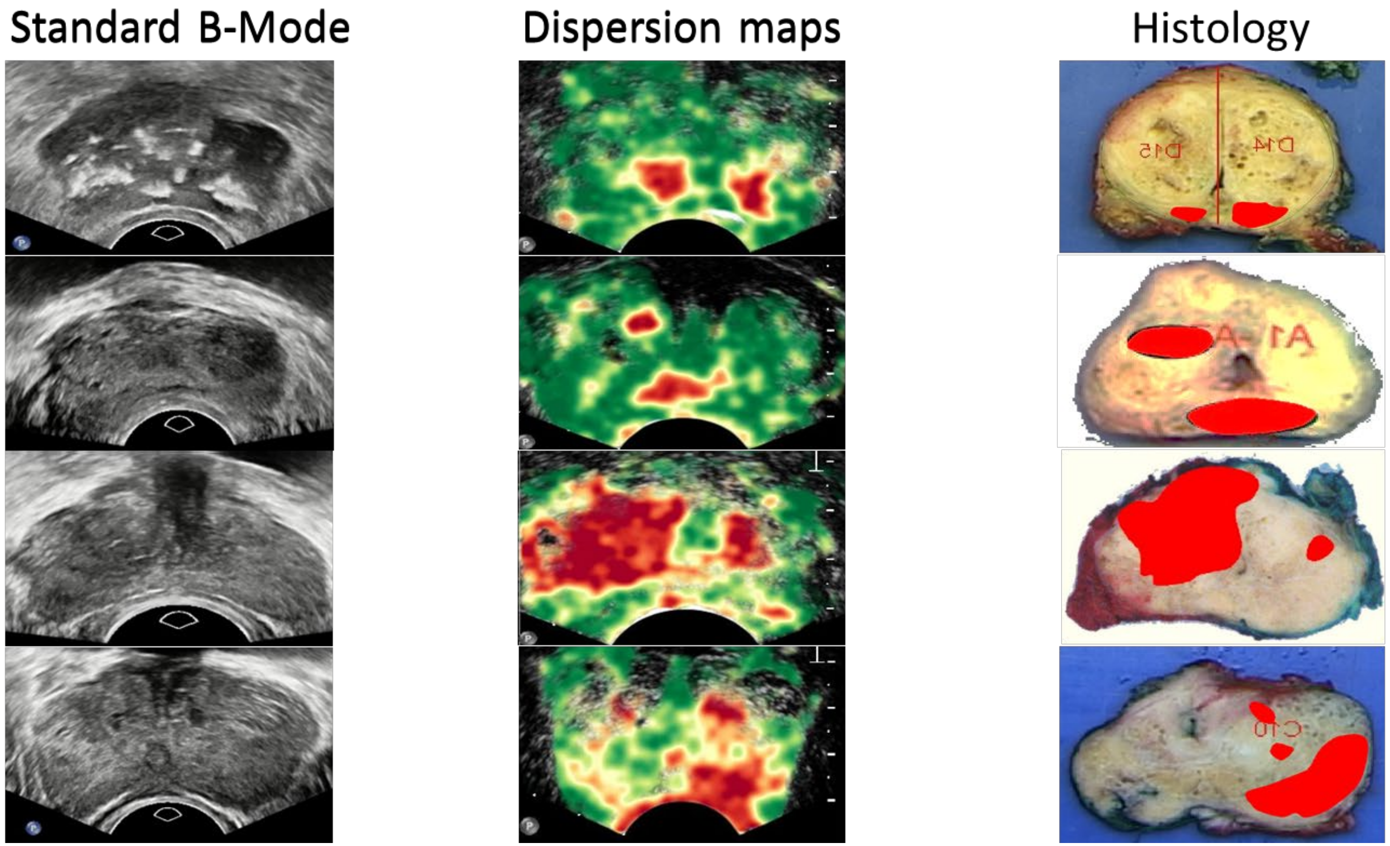

CUDI targeted biopsies

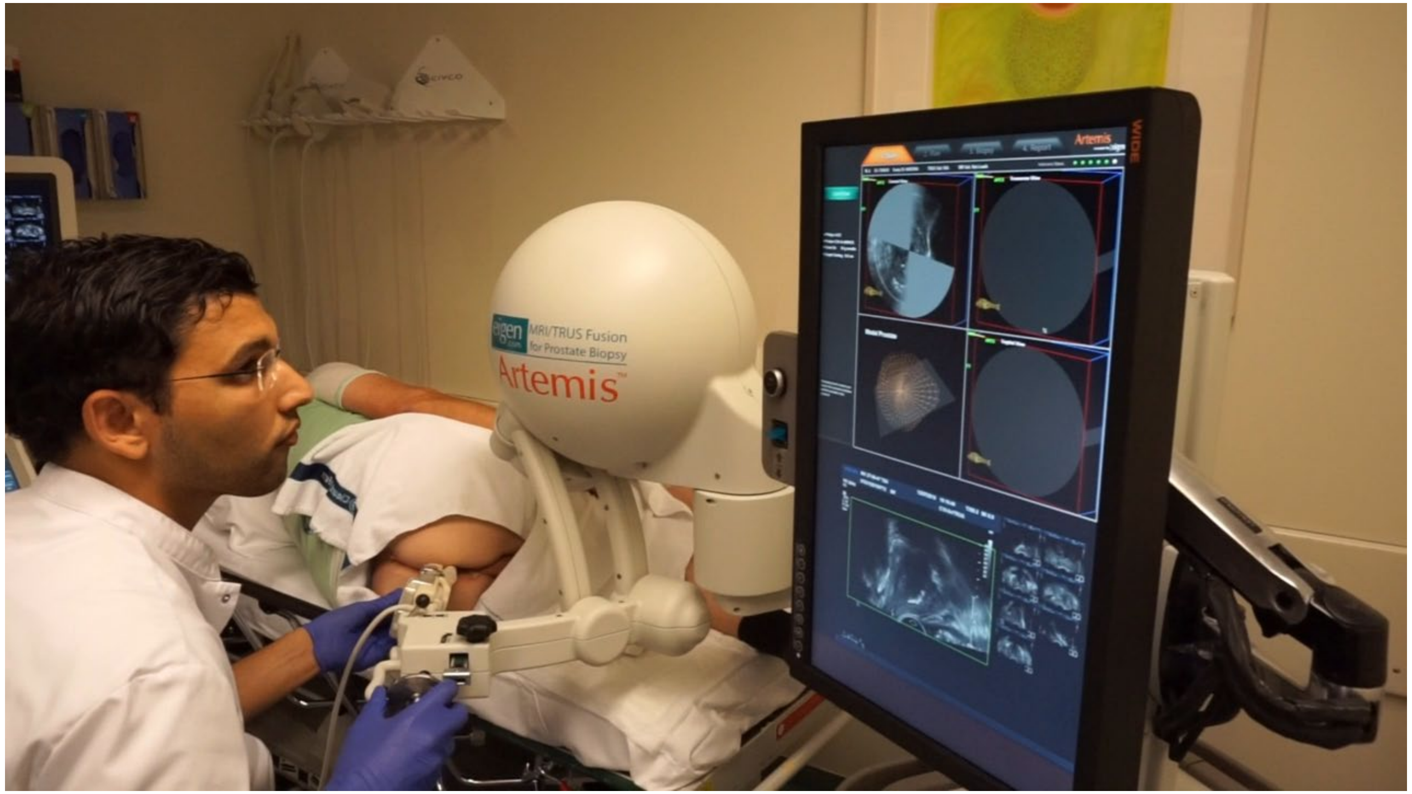

Biopsies targeted by CUDI compared to systematic biopsy and mpMRI targeted biopsies in <u>142 patients</u>

Detection rates csPCa:

SBx = 39% (56/142)

mpMRI-TBx = 29% (41/142)

CUDI-TBx = 28% (40/142)

Mannaerts et al. *BJUI* 2020

2D multiparametric ultrasound (mpUS)

Martini-Klinik
Prostatakrebszentrum
Universitätsklinikum Hamburg-Eppendorf

Mannaerts et al. *BMC Urology* 2018
Mannaerts et al. *J Urology* 2019

Multiparametric ultrasound in the detection of prostate cancer: a systematic review

Arnoud Postema · Massimo Mischi · Jean de la Rosette · Hessel Wijkstra

World J Urol (2015) 33:1651–1659 1655

GSU, C-TRUS, DCE-US and SWE are expected to show improved results in the near future. By effectively combining these ultrasound techniques, all targeting different properties of malignant tissue, a valuable clinical tool with all the advantages of ultrasound could be constructed. The literature shows that combining ultrasound modalities in a crude fashion can already improve sensitivity by 13–59 %.

DCE-US	Seitz et al. [33]	35	DCE-US versus RP and RCP	69	33	84	18
	Unpublished data from AMC	36	DCE-US + GSU versus RP	58–69	93–95		
	Unpublished data from AMC	11	Semiquantative DCE-US + GSU versus RP	87	84		
	Jung et al. [41]	20	Semiquantitative DCE-US versus RP	88	100		
SE	Zhang et al. [44]	508	Meta-analysis of 7 studies: SE versus RP	72	76		
	Teng et al. [45]	527	Meta-analysis: SE-targeted biopsy versus systematic biopsy	62	79		
SWE	Ahmad et al. [49]	50	Per ROI SWE versus 12 biopsies	90–93	88–93	93–98	83–81
	Barr et al. [48]	53	Per ROI SWE versus 12 biopsies	96	96	69	100

48 patients

B-Mode, CUDI, SWE

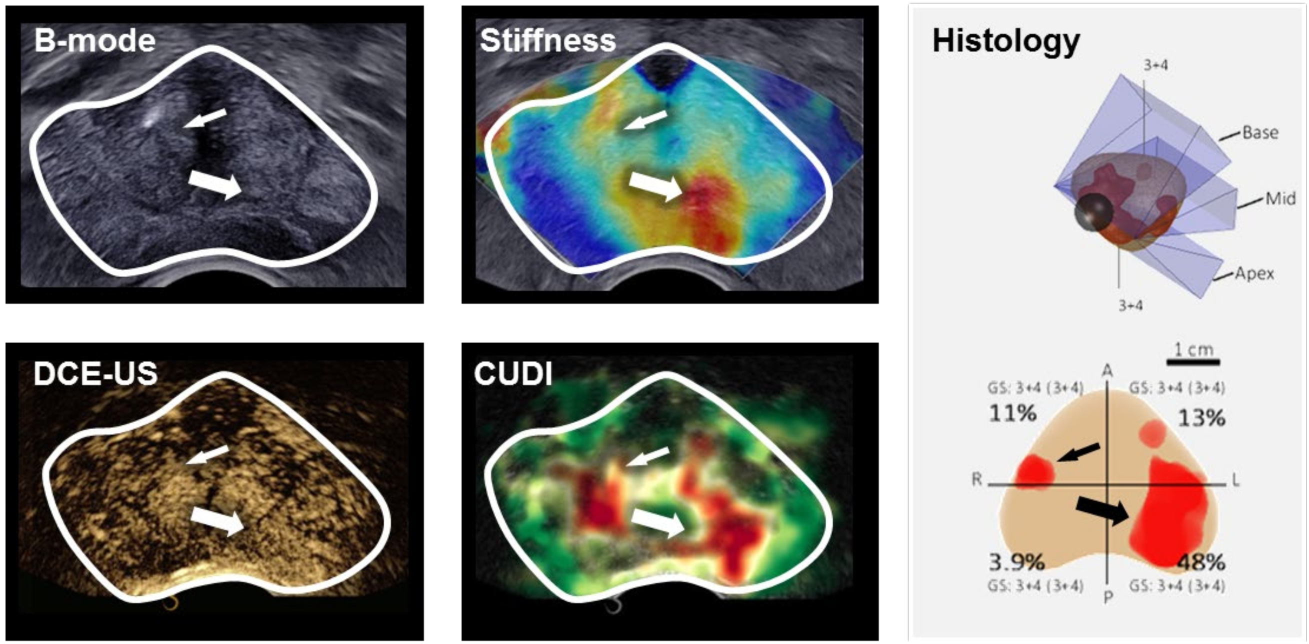

Automatic zonal segmentation by deep learning

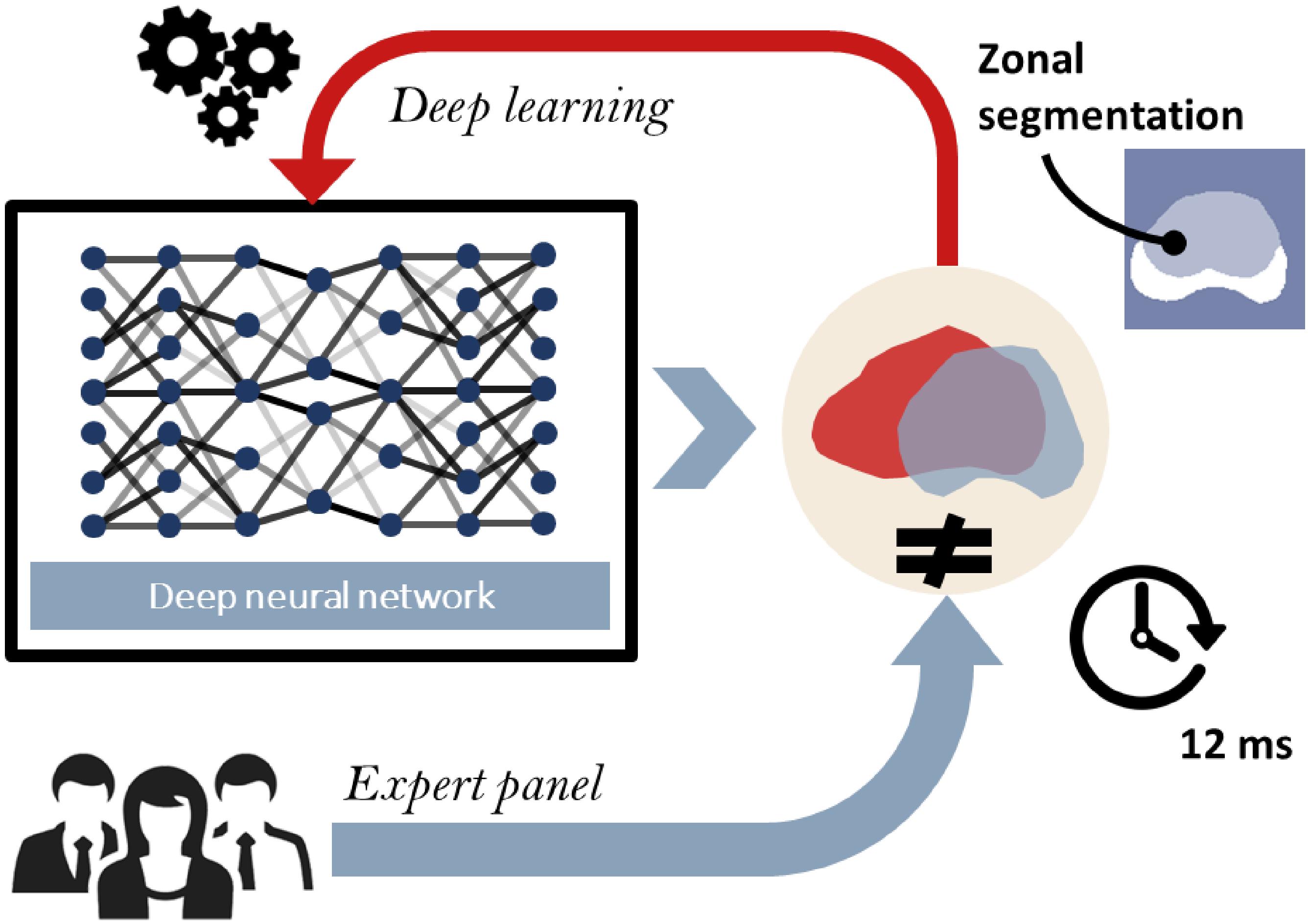

van Sloun et al. *Eur Urol Focus* 2019

2D multiparametric ultrasound (mpUS)

Martini-Klinik
Prostatakrebszentrum
Universitätsklinikum Hamburg-Eppendorf

Mannaerts et al. *BMC Urology* 2018
Mannaerts et al. *J Urology* 2019

Machine learning

(Random forest classifier)

48 patients

B-Mode, CUDI, SWE

Mode	Parameter	ROC-AUC per region	
		≥3+3	>3+4
B-mode	*G*, gray level	0.53	0.58
SWE	*E*, Young's modulus	0.62	0.73
DCE-US	*v*, contrast velocity (mm/s)	0.69	0.76
	r, similarity dispersion(-)	0.69	0.76
	PT, time to peak (s)	0.63	0.68
	Multi-Radiomic *v*	0.71	0.84
RF-classifier	Multiparametric score	0.75	0.90

Wildeboer et al. *Eur Radiol* 2019

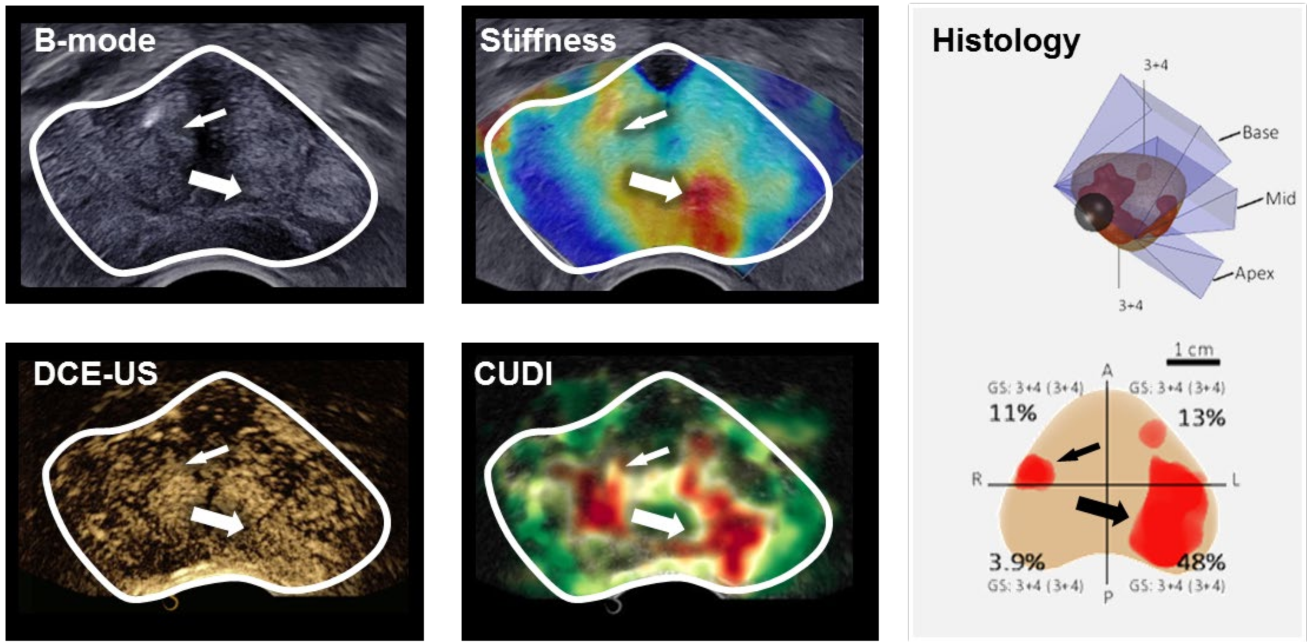

3D CUDI

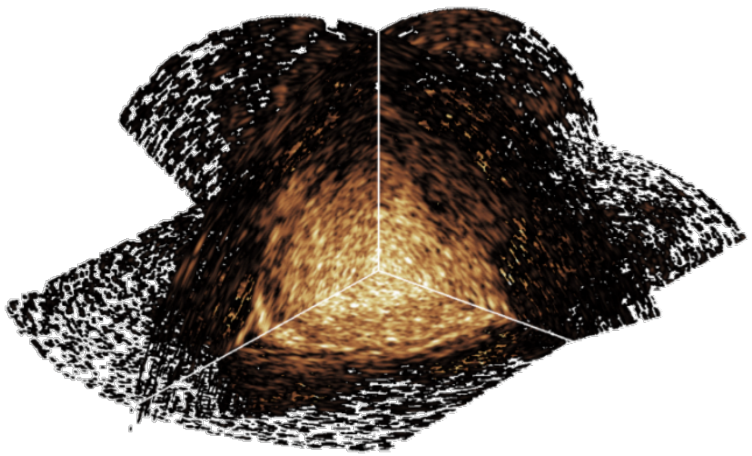

Advantages

- Entire gland in one go
- Faster clinical workflow
- Complete kinetic modeling

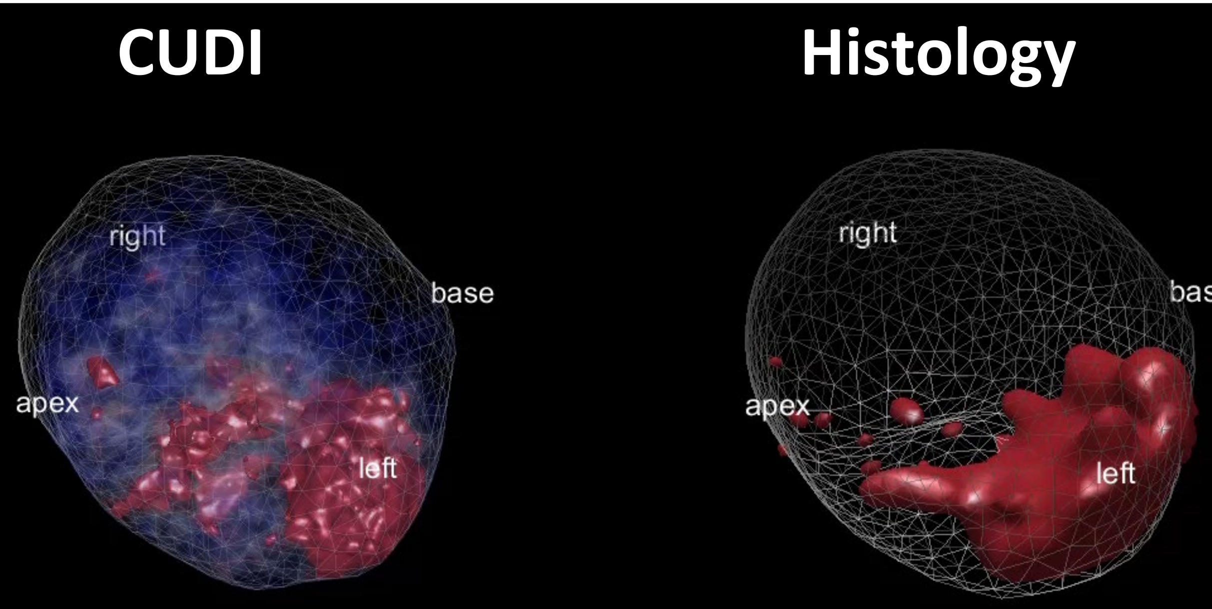

Schalk et al. *IEEE T-UFFC* 2015; Schalk et al. *UMB* 2018
Wildeboer et al. *IEEE T-MI* 2018; Wildeboer et al. *UMB* 2019

3D CUDI

Vascular reconstruction by tractography

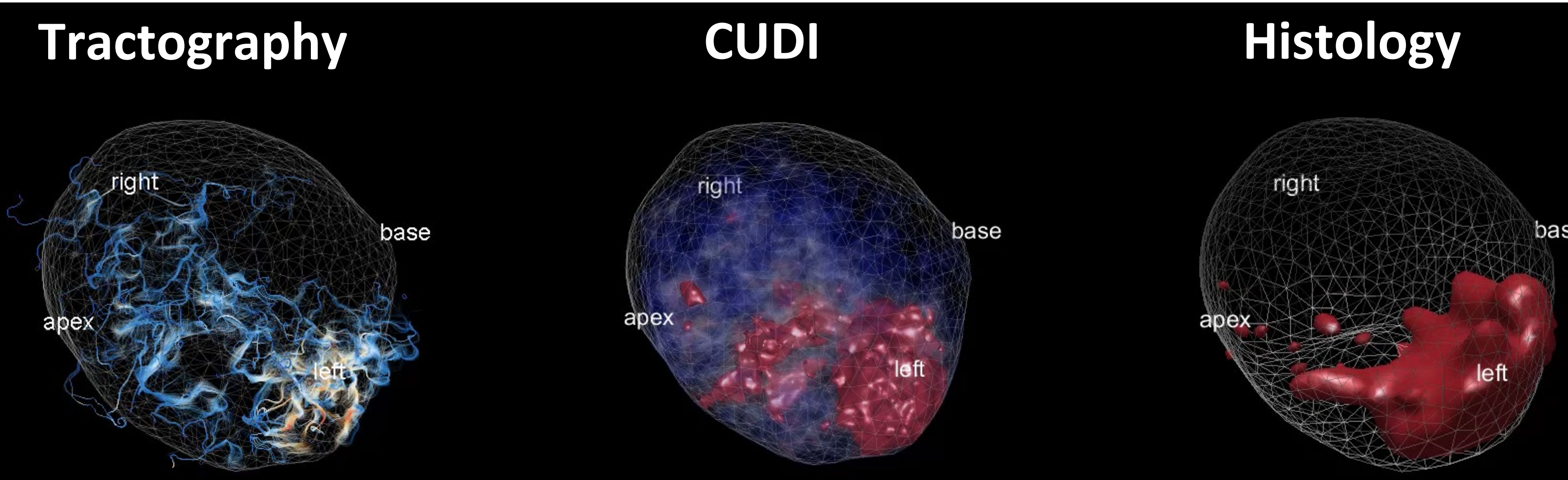

van Sloun et al. *Nature Scientific Reports* 2018

3D mpUS: prediction of biopsy outcome

54 patients compared to 12-core SBx

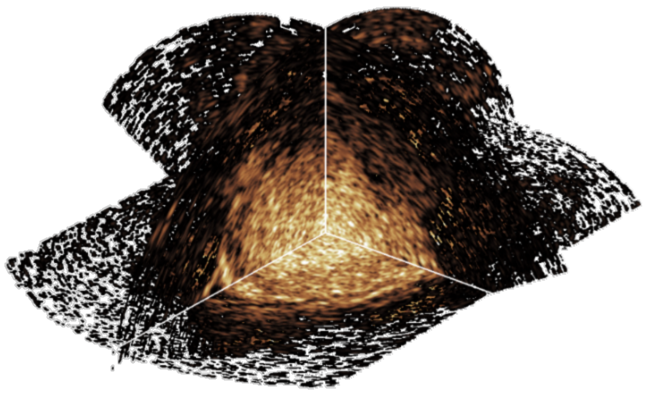

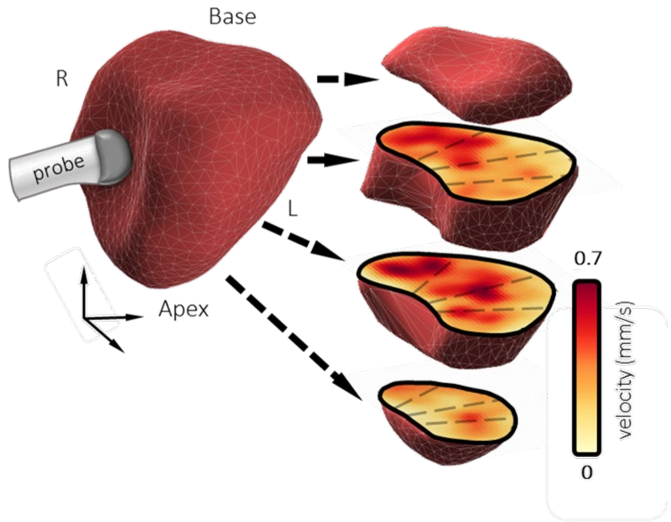

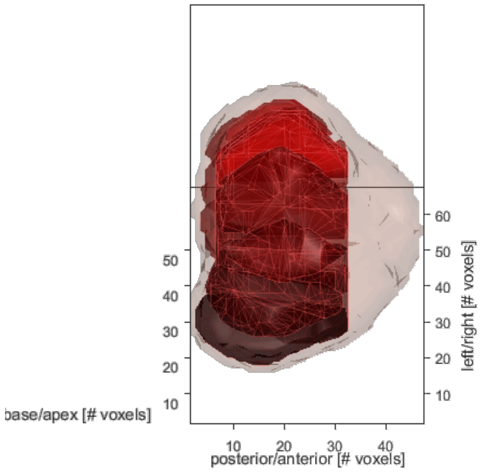

Features

- B-Mode – LogiqE9 (RIC9-5 probe)
- CUDI – LogiqE9 (0.3 Hz, MI = 0.1, 2.4 mL SonoVue)
- SWE – Aixplorer (multiplane 3D reconstruction)

Chen et al. *IEEE IUS* 2021

3D mpUS: prediction of biopsy outcome

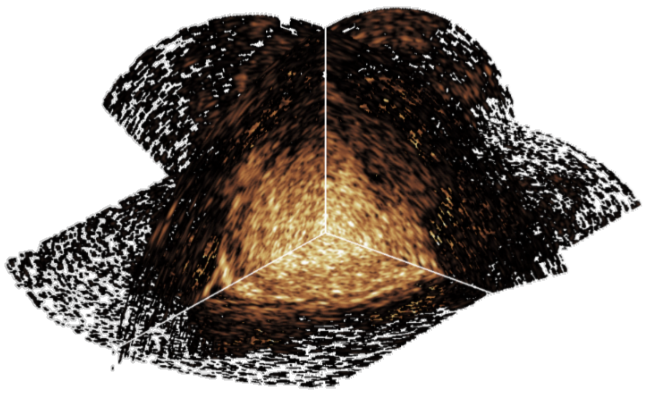

54 patients compared to 12-core SBx

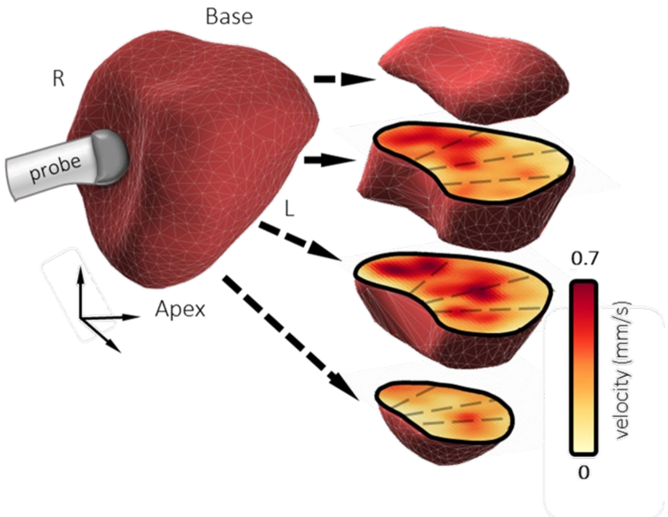

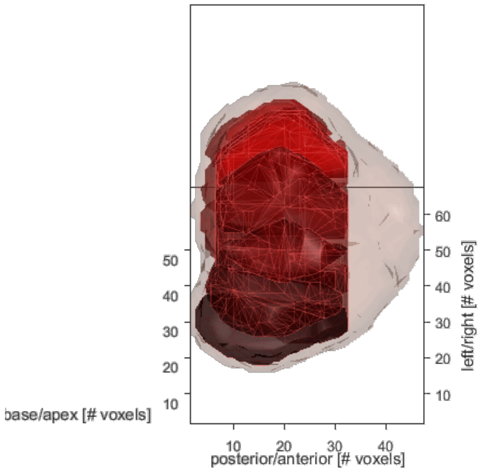

Features
- B-Mode
- CUDI
- SWE

Machine learning

(Gradient boosting)

	ROC curve area*
CUDI	**0.81 ± 0.12**
SWE	**0.66 ± 0.12**
CUDI + SWE	**0.85 ± 0.11**

*9-fold cross validation

Chen et al. *Euroson* 2022

Breast cancer data – 2D CEUS

MEDICAL UNIVERSITY OF VIENNA

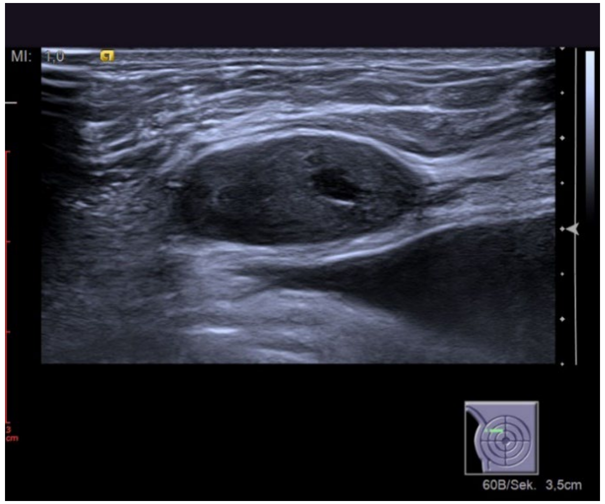

B-mode

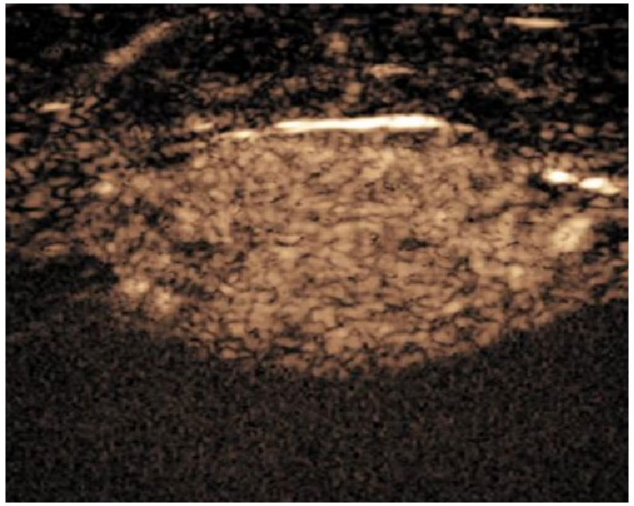

CEUS

- 120 patients (18-82 years, average: 52 years)
- B-Mode + CEUS + biopsy
- October 2015 - September 2016

CEUS setting

- Siemens Acuson S3000
- Linear transducer (9L4HD)
- CPS at 4 MHz
- MI ≤ 0.07
- 4.8-mL bolus of SonoVue

Enhancement heterogeneity

Benign breast lesion with
low enhancement heterogeneity

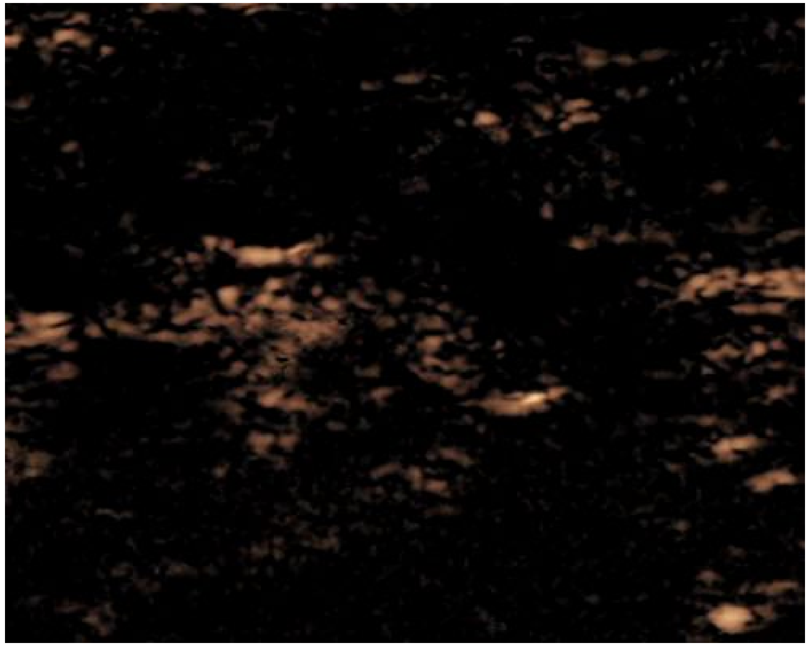

Malignant breast lesion with
high enhancement heterogeneity

CEUS enhancement grade

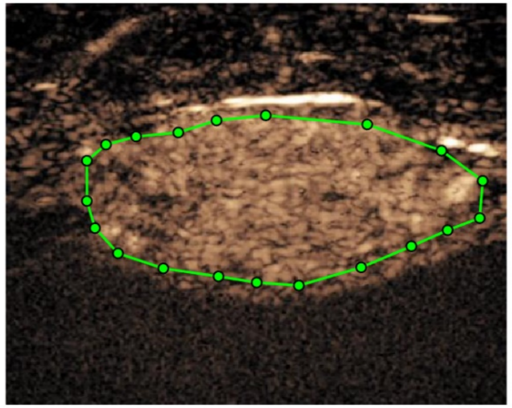
Grade 1, Hyper-enhanced

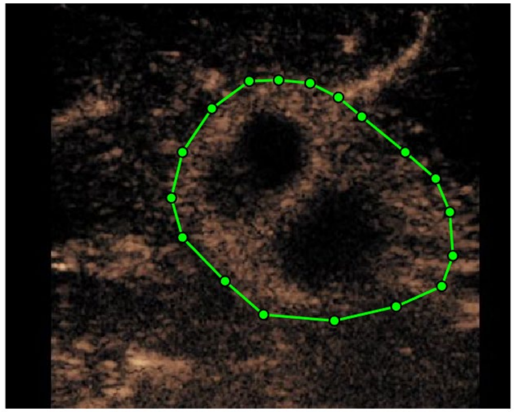
Grade 2, Partly enhanced

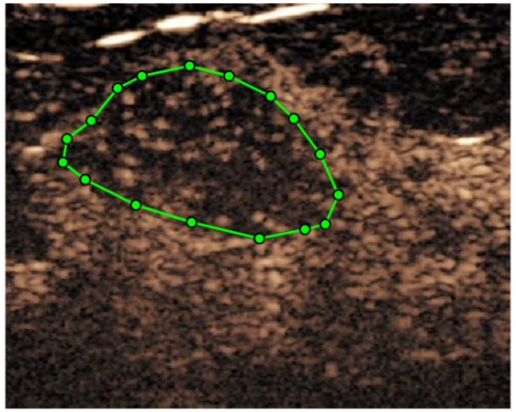
Grade 3, Poorly enhanced

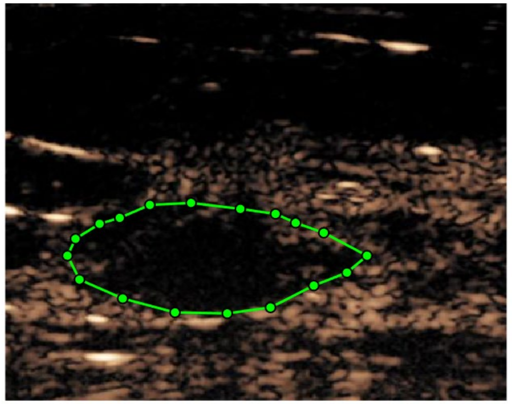
Grade 4, Hypo-enhanced

Quantitative enhancement grading
- Enhancement ratio*
- Average enhancement*

*At peak enhancement

CUDI spatiotemporal analysis of CEUS loops

Similarity between time intensity curves (TICs)

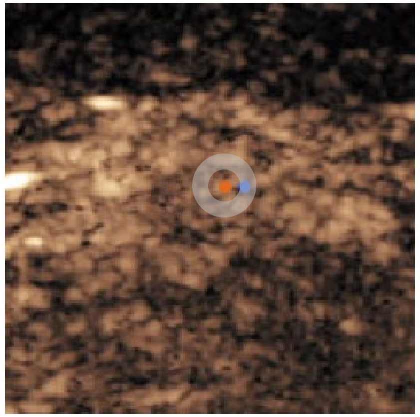

1.5 cm × 1.5 cm

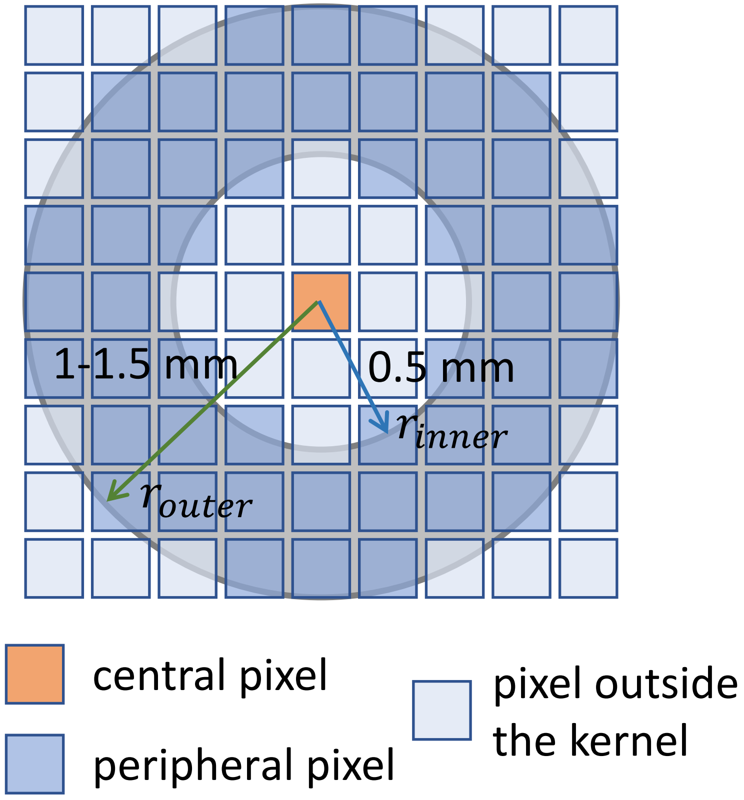

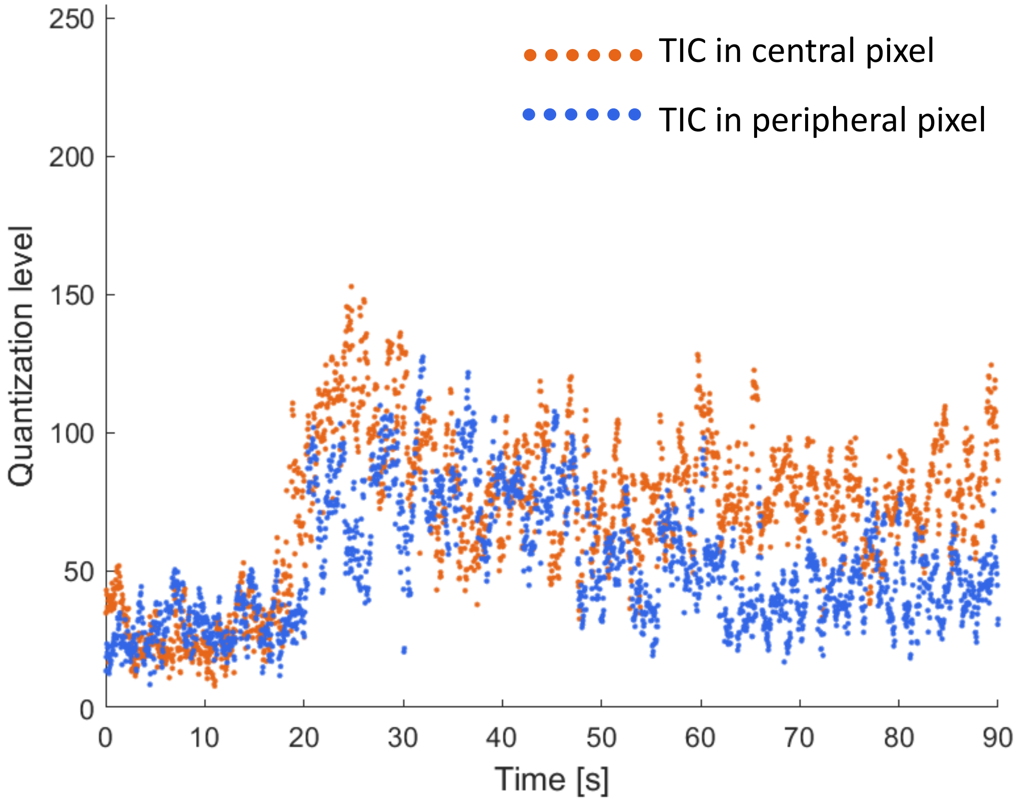

CUDI spatiotemporal analysis of CEUS loops

Similarity between time intensity curves (TICs)

Spectral coherence (ρ)

Mischi et al. *IEEE TUFFC* 2012

Kuenen et al. *UMB* 2013

Correlation coefficient (r)

Kuenen et al. *IEEE TUFFC* 2013

Mutual information (I)

Schalk et al. *IEEE TBME* 2016

$$I = \sum_{c \in Q} \sum_{\boldsymbol{x} \in \boldsymbol{Q}} P_{\boldsymbol{X},C}(\boldsymbol{x}, c) \log\left(\frac{P_{\boldsymbol{X},C}(\boldsymbol{x}, c)}{P_C(c) P_{\boldsymbol{X}}(\boldsymbol{x})}\right)$$

Conditional entropy (H)

$$H = -\sum_{c \in Q} \sum_{\boldsymbol{x} \in \boldsymbol{Q}} P_{\boldsymbol{X},C}(\boldsymbol{x}, c) \log\left(\frac{P_{\boldsymbol{X},C}(\boldsymbol{x}, c)}{P_{\boldsymbol{X}}(\boldsymbol{x})}\right)$$

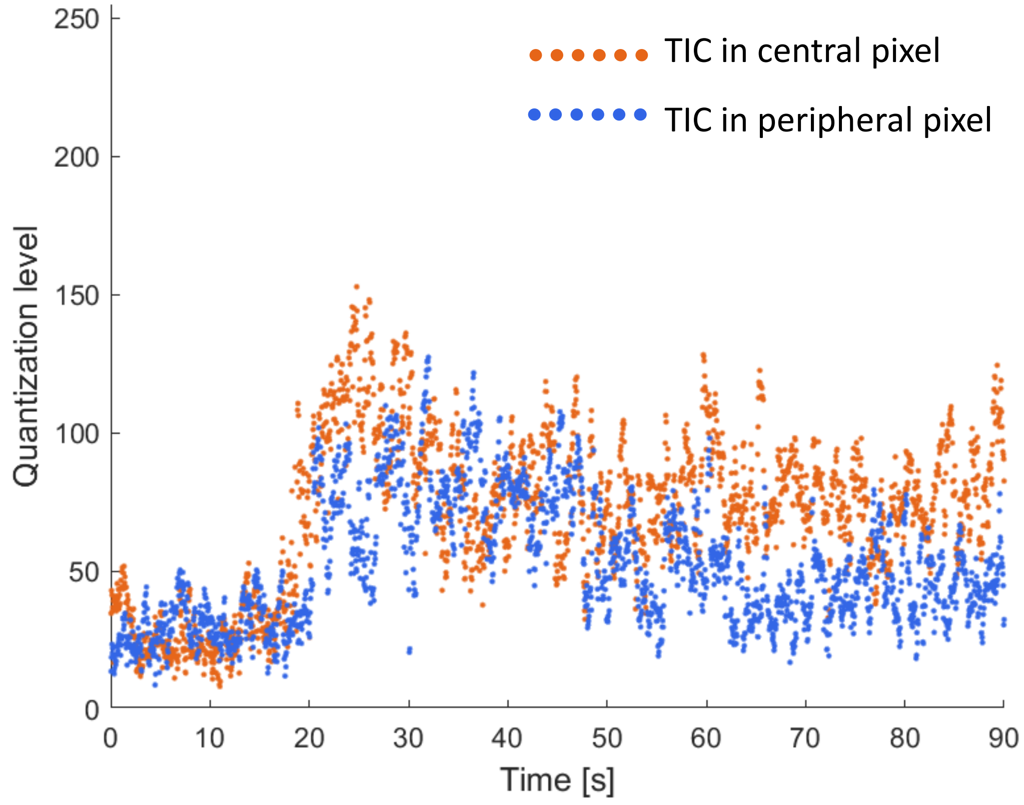

Results - Mutual Information

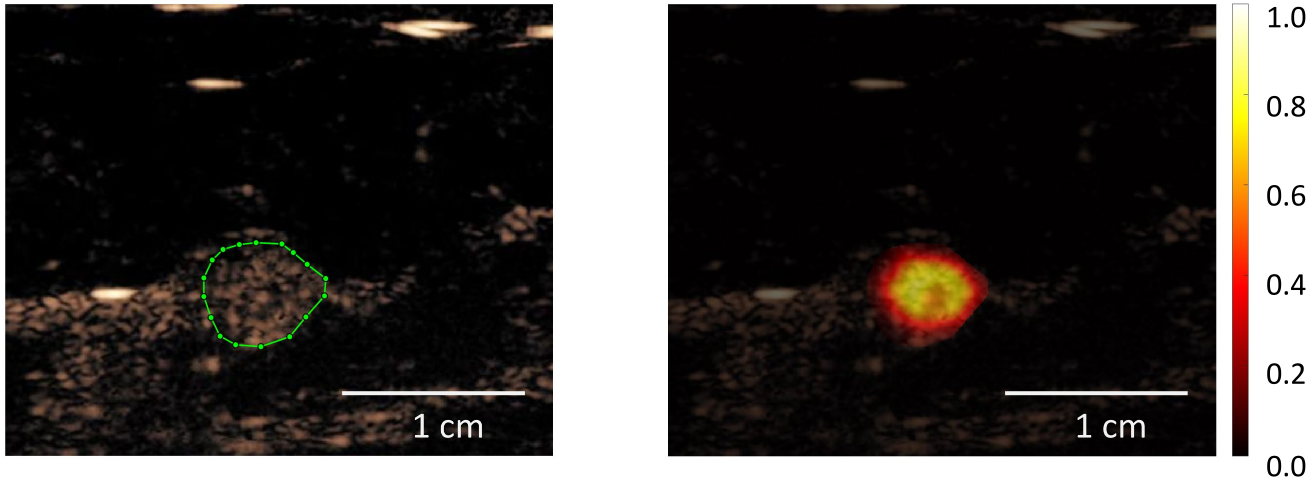

6-mm benign ductal hyperplasia in a 60-year-old woman

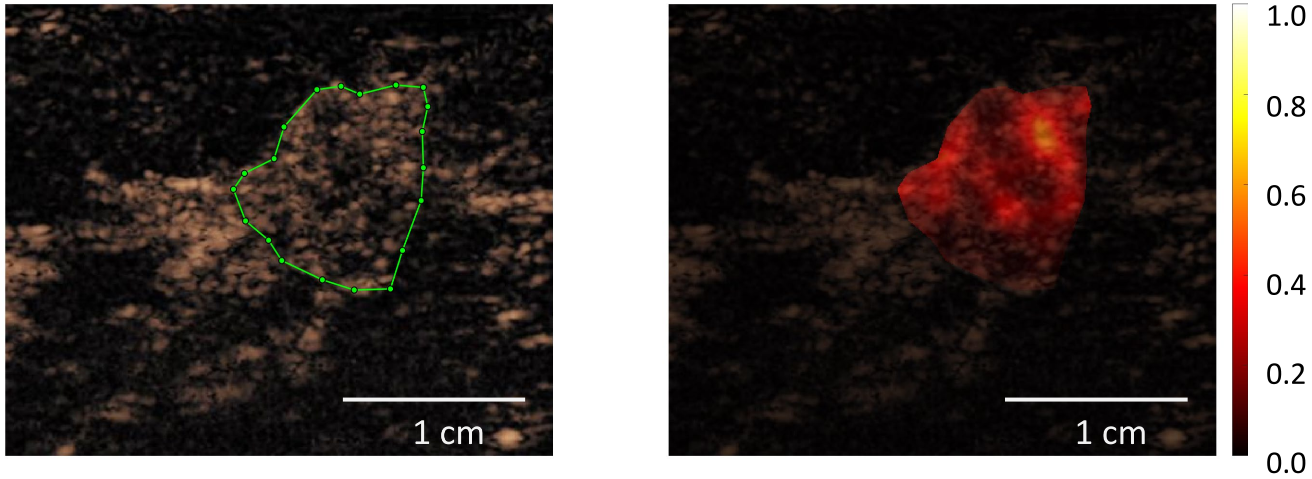

10-mm malignant invasive ductal carcinoma in a 43-year-old woman

Results - pixel level classification

Grade 1

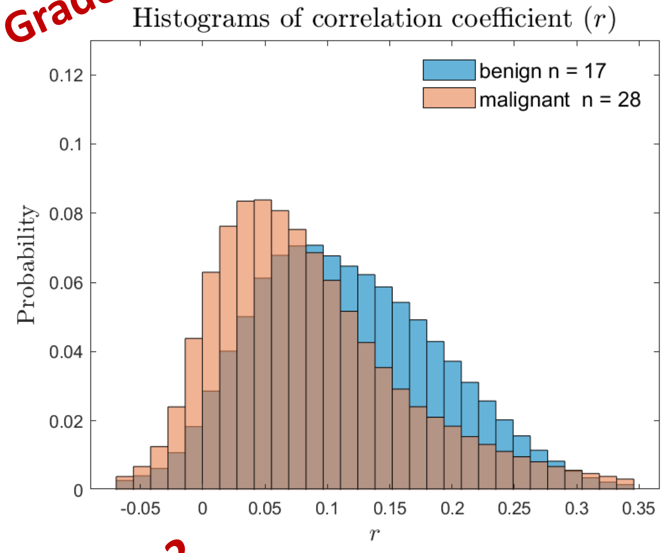

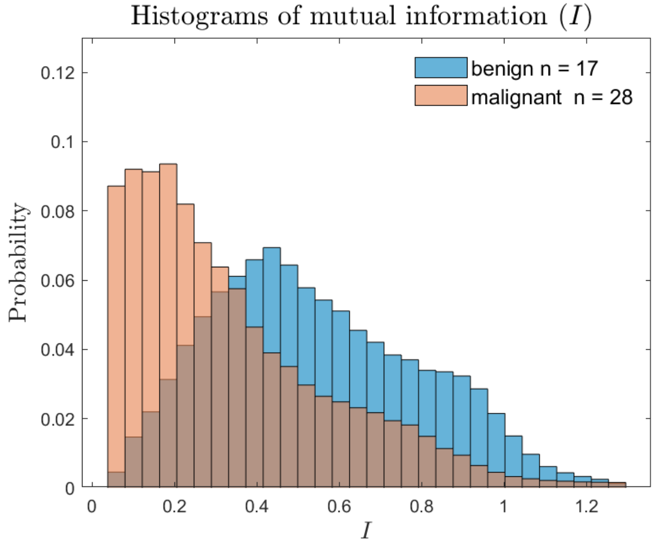

Grade 1+2

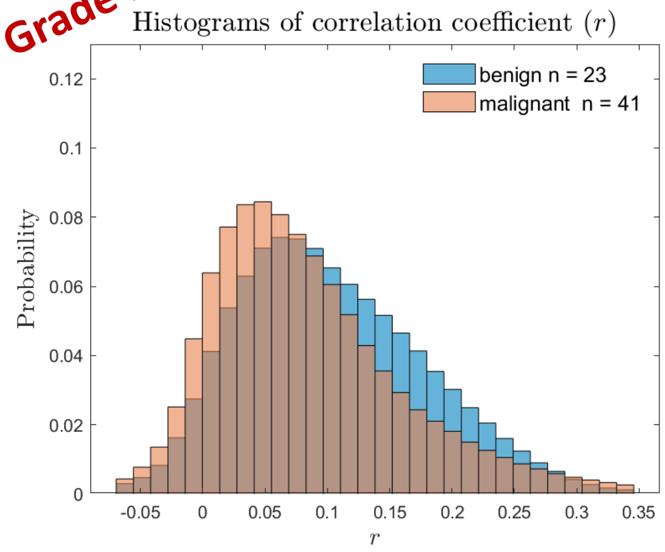

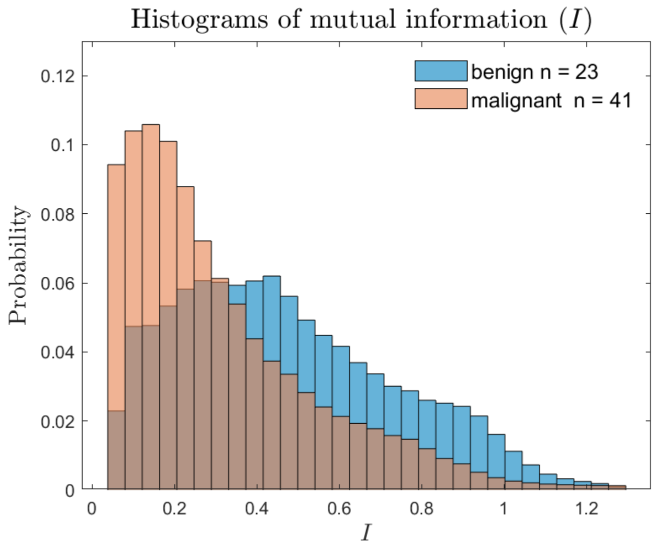

Statistics of parameter difference at the pixel level

	Parameter	Benign	Malignant	p value
Patients of grade 1 (45/120)	Correlation coefficient (r)	0.115 ± 0.077	0.088 ± 0.082	0.043
	Spectral coherence (ρ)	0.478 ± 0.201	0.416 ± 0.222	0.127
	Mutual information (I)	0.547 ± 0.253	0.478 ± 0.201	<0.001
	Conditional entropy (H)	5. 263 ± 0.357	5.525 ± 0.315	<0.001
Grouped patients of grade 1 or 2 64/120	Correlation coefficient (r)	0.103 ± 0.076	0.085 ± 0.080	0.189
	Spectral coherence (ρ)	0.441 ± 0.208	0.412 ± 0.216	0.362
	Mutual information (I)	0.473 ± 0.266	0.322 ± 0.252	0.002
	Conditional entropy (H)	5.351 ± 0.359	5.543 ± 0.299	0.002

Results - Lesion classification

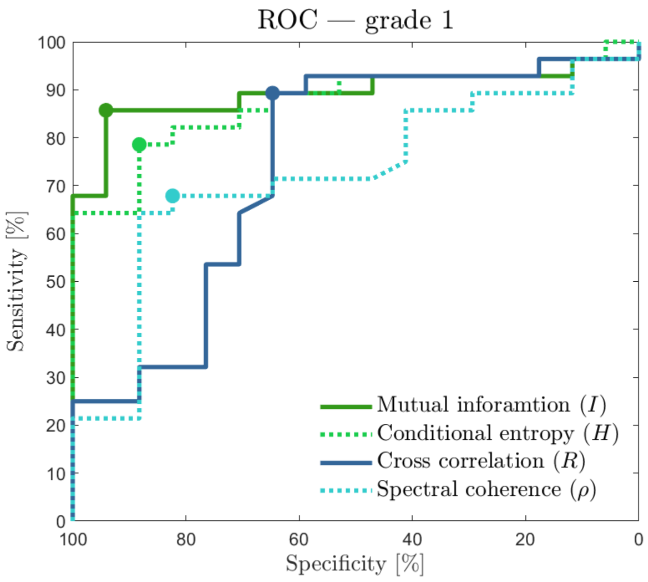

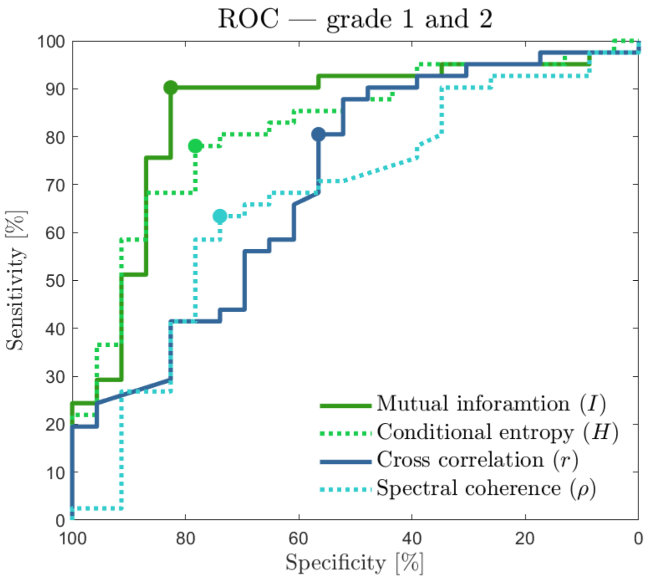

Table 3 Comparison of diagnostic performance of spatiotemporal parameters

	Parameter	Sensitivity (95% CI)	Specificity (95% CI)	AUC	P value
Lesions of grade 1 (45/120)	Correlation coefficient (r)	89.3% (72.5 96.9)	64.7% (40.5 86.7)	0.743	0.010
	Spectral coherence (ρ)	67.9% (48.3 82.7)	82.3% (57.3 100)	0.724	0.015
	Mutual information (I)	85.7% (68.2 96.4)	94.4% (68.8 100)	0.893	<0.001
	Conditional entropy (H)	78.6% (60.8 92.9)	88.2% (41.7 100)	0.874	<0.001
Grouped lesions of grade 1 or 2 (64/120)	Correlation coefficient (r)	80.5% (66.7 90.5)	66.5% (37.8 75.0)	0.704	0.008
	Spectral coherence (ρ)	63.4% (48.2 76.3)	75.9% (53.0 91.7)	0.670	0.034
	Mutual information (I)	90.2% (79.6 97.5)	82.6% (61.2 94.5)	0.848	<0.001
	Conditional entropy (H)	78.1% (62.6 89.7)	78.3% (56.0 90.0)	0.817	<0.001

Conclusions

- CUDI spatiotemporal analysis of enhancing breast lesions (64/120) shows good classification performance, especially by mutual information (AUC=84.8%, Se=90.2%, Sp=82.6%)
- More quantitative parameters should be evaluated that reflect the complex perfusion patterns in breast lesions
- Hypoenhancing lesions call for a multiparametric approach involving other complementary features (texture, geometry, stiffness)
- 3D CEUS is expected to provide more accurate classification with motion compensation

Thank you!

Special acknowledgements:
Panagiotis Kapetas (Medical University of Vienna)
Chuan Chen (Eindhoven University of Technology)
Simona Turco (Eindhoven University of Technology)
Hessel Wijkstra (Eindhoven University of Technology)
Chris de Korte (Radboudumc)
Ritse Mann (Radboudumc)

PhD students


Maarten Kuenen
(TU/e)


Stefan Schalk
(TU/e)


Simona Turco
(TU/e)


Ruud van Sloun
(TU/e)


Rogier Wildeboer
(TU/e)


Peiran Chen
(TU/e)


Martijn Smeenge
(AMC)


Arnoud Postema
(AMC)


Maudy Gayet
(TU/e - JBZ)


Christophe Mannaerts
(AMC)


Auke Jager
(AMC)

THE 2022
TECHMED
EVENT